From Molecular Aggregation to a One-Dimensional Quantum Crystal of Deuterium Inside a 1-nm Carbon Nanotube

María Pilar de Lara-Castells*,† and Alexander O. Mitrushchenkov*,‡

†*Instituto de Física Fundamental (AbinitSim Unit), CSIC, Serrano 123, 28006 Madrid, Spain*

‡*MSME, Univ Gustave Eiffel, UPEC, CNRS, F-77454, Marne-la-Vallée, France.*

E-mail: Pilar.deLara.Castells@csic.es; Alexander.Mitrushchenkov@univ-eiffel.fr

Abstract

The quantum motion of clusters of up to four deuterium molecules under confinement in a single-wall (1-nm diameter) carbon nanotube is investigated by applying a highly accurate full quantum treatment of the most relevant nuclear degrees of freedom and an *ab initio*-derived potential model of the underlying dispersion-dominated intermolecular interactions. The wavefunctions and energies are calculated using an *ad-hoc*-developed discrete-variable-representation (DVR) numerical approach in internal coordinates, with the space grid approaching a few billions of grid points. We unambiguously predict the formation of a solid-like pyramidal one-dimensional chain structure of molecules under the cylindrical nanotube confinement. The onset of solid-like packing is explained by analyzing the potential minima landscape. The stabilization of collective rotational motion through "rigid rotations" of four deuterium molecules provides conclusive evidence for the onset of a quantum solid-like behaviour resembling that of quantum rings featuring persistent current (charged particles) or persistent flow (neutral particles).

Graphical TOC Entry

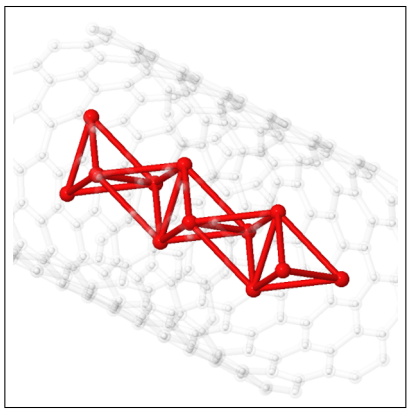

As the lightest molecule in nature, frozen molecular hydrogen (or deuterium) is a paradigmatic case of a molecular quantum crystal,[1] with the molecules being held together by weak dispersion forces. The cylindrical confinement provided by carbon nanotubes has offered the possibility of studying this quantum system at reduced dimensionality. Particularly, the quest for the occurrence or either quasi-superfluid or quasi-crystalline behavior of para-hydrogen molecules when confined in armchair carbon nanotubes has recently motivated an intense, somewhat controversial, theoretical research.[2–4] From a practical perspective, high surface area and precisely tuned pores of carbon nanotubes have rendered them relevant materials for efficient hydrogen storage. Since the general goal in hydrogen storage methods is to pack hydrogen molecules as close as possible, the likehood for solid-like packing of hydrogen in carbon-based nanoporous materials has drawn considerable attention, existing experimental evidences at supercritical temperatures of industrial importance.[5] In the case of molecular deuterium, our recent theoretical work have indicated the possibility for hexagonal-close-packing (as in the bulk phase) of D_2 molecules inside an armchair carbon nanotube of helicity index (10,10).[6] As observed for helium under carbon nanotube confinement,[7, 8] all these studies[2–4, 6] have highlighted the key role played by the quantum nature of the nuclear degrees of freedom in the confined hydrogen or deuterium motion.

This work is aimed to accurately characterize the transition from molecular aggregation to solid-like packing of deuterium molecules inside the single-wall (1-nm) carbon nanotube (SWCNT) with helicity index (11,4) represented in Fig. 1 (left panel). To provide conclusive evidence on the quantum nature of the solid-like system, we also analyse the stabilization of excited collective rotational states. The presence of these states as minima in the energy spectrum as a function of the angular momentum has been previously interpreted with the onset for superfluidiy and persistent flow of bosonic particles in a ring by Bloch.[9] The same analysis allowed us to provide insight into experimental measurements[10–12] attributed to a superfluid behaviour in doped para-hydrogen clusters.[13] In order to consider a nanotube as the "dopant" species instead of a molecule, we have extended and improved our *ad-hoc*-developed full quantum approach of the D_2 molecular motion of Ref. 6. This refinement makes possible to consider explicitly the number of molecules which are necessary for the onset of a quantum solid-like behavior while an embedding treatment was employed in our previous study for the same purpose.[6] The approach is routed on our nuclear orbital method followed by Full Configuration Interaction diagonalization (FCI-NO)[13–17] but with the Hamiltonian recast in internal coordinates. Its key advantage over quantum Monte Carlo treatments is due to its capability to deliver excited states with similar accuracy to the ground state.

To achieve a consistently accurate description of the D_2–SWCNT(11,4) interaction, we have employed our *ab initio*-derived pairwise additive potential model.[6] For the concrete case of van-der-Waals-dominated adsorbate/(carbon-based) surface interactions, [6, 18–20] its adequacy relies on the excellent transferability properties found for the parameters accounting for the dispersion contribution upon increasing the size of clusters modelling the extended systems.[19] Complicated, dispersionless contributions are mostly of short-range nature and the usage of small cluster models can be also justified. Therefore, different analytical forms are employed to model the dispersionless and dispersion contributions, with the model parameters being computed at *ab initio* level on a short and narrow carbon nanotube and then scaled to the actual system. The detailed energy decomposition offered by the symmetry-adapted perturbation theory approach[21, 22] has rendered such strategy successful when describing the adsorption of molecular and atomic species to the carbon material[6, 18, 23] (see section S1 of the supporting information for details of the potential model).

To describe the quantum motion of N D_2 molecules inside the nanotube, an earlier developed "pseudo-particle" approach[6, 13] is ap-

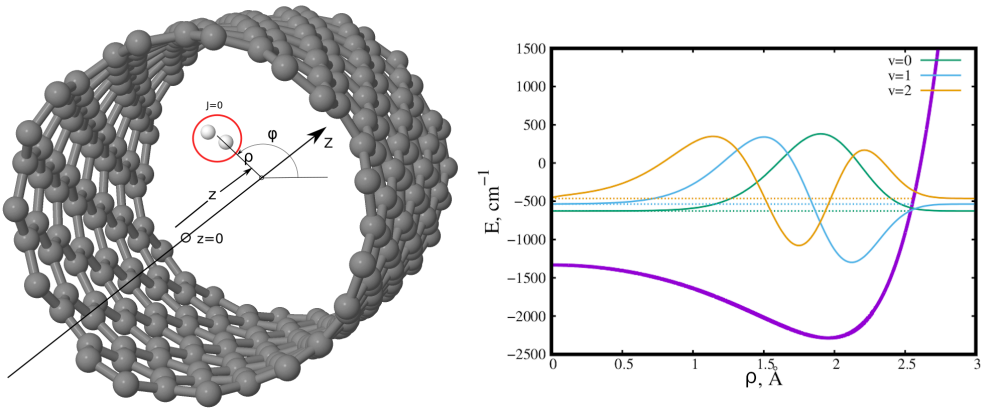

Figure 1: Left panel: Figure illustrating the atomic structural model of the D_2/SWCNT system. Gray spheres represent carbon atoms while blue spheres stand for one D_2 molecule inside a 1-nm carbon nanotube of helicity index (11,4). Cylindrical coordinates (ρ, ϕ, z) of the D_2 center-of-mass are also indicated. Right panel: Representation of the D_2–SWCNT interaction (shown in violet) and the three lowest-lying energy states of the $D_2 \subset$ SWCNT(11,4) system.

plied by representing the molecules as heavy point-like bosonic particles. This "pseudo-particle" approach has been successfully employed in previous studies of the H_2 graphene interaction.[24, 25] The nanotube is considered as infinite, structureless, and fixed in the space environment. In this way, the interaction between the nanotube and a given molecule $V_1(\rho)$ depends only on the distance between the molecule center-of-mass (COM) and the nanotube center ρ (see Fig. 1). As previously shown,[6, 23] the Z dependence of the interaction (i.e., along the wire), or Φ (referred to as the overall rotation coordinate) can be neglected in a first approximation. Under these constraints, the effective Hamiltonian is expressed as

$$H_N = \sum_{i=1}^{N} \left\{ -\frac{1}{2M}\Delta(\mathbf{r}_i) + V_1(\rho_i) \right\} + \sum_{i<j} V_2(r_{ij}),$$

with M being the mass of a single D_2 molecule. Since the motion of the $(D_2)_N$ center-of-mass leads to a continuum spectrum, the Hamiltonian has to be recast in internal coordinates which do not contain the overall Z-translation. Moreover, we can also separate the overall rotation so that the internal Hamiltonian will depend on $3N-2$ coordinates, having a parametric dependence of the overall rotation quantum number (referred to as Λ). In order to calculate the wavefunction of the $(D_2)_N \subset$ SWCNT system in internal coordinates, we first introduce cylindrical coordinates for each particle, $x, y, z \rightarrow \rho, \phi, z$ and perform a Jacobian transformation of the wavefunction. The one-particle kinetic energy is then given by

$$-\frac{1}{2M}\Delta(\mathbf{r}) = -\frac{1}{2M}\left\{ \frac{\partial^2}{\partial\rho^2} + \frac{\partial^2}{\partial z^2} + \frac{1}{\rho^2}\left[\frac{\partial^2}{\partial\phi^2} + \frac{1}{4} \right] \right\}.$$

The two-particle interaction V_2 is written in cylindrical coordinates by using the expression,

$$r_{ij}^2 = \rho_i^2 + \rho_i^2 + (z_i - z_j)^2 - 2\rho_i\rho_j\cos(\phi_i - \phi_j)$$

To separate the overall Z-translation and overall rotational motions, we introduce relative coordinates as $t_i = z_i - z_N$ and $\chi_i = \phi_i - \phi_N$, for $i = 1 \ldots N-1$. The overall Z-translation and overall rotation coordinates are conveniently defined as $Z = Z_{\mathrm{COM}} = \frac{1}{N}\sum_{i=1}^{N} z_i$ and $\Phi = \phi_N$. The overall rotation quantum number reads $\Lambda = m_1 + m_2 + \cdots + m_N$, where m_i is the integer standing for the projection of the angular momentum of the i-th particle onto the nanotube axis. Since both D_2–SWCNT and D_2–D_2 interactions do not depend on Φ, the coordinate Φ can be separated via the factor $\exp(i\Lambda\Phi)\Psi(\chi_i)/\sqrt{2\pi}$. Finally, the full kinetic energy is written as $K_N = -\frac{1}{2M}\sum_{i=1}^{N}\Delta(\mathbf{r}_i) =$

$K_N(z) + K_N(\rho) + K_N(\phi)$ where

$$K_N(z) = -\frac{1}{M}\sum_{i=1}^{N-1}\frac{\partial^2}{\partial t_i^2} - \frac{1}{M}\sum_{i<j=1}^{N-1}\frac{\partial}{\partial t_i}\frac{\partial}{\partial t_j}$$

$$K_N(\rho) = -\frac{1}{2M}\sum_{i=1}^{N}\frac{\partial^2}{\partial \rho_i^2}$$

and

$$K_N(\phi) = -\frac{1}{2M}\sum_{i=1}^{N-1}\frac{1}{\rho_i^2}\left[\frac{\partial^2}{\partial \chi_i^2} + \frac{1}{4}\right]$$
$$-\frac{1}{2M}\frac{1}{\rho_N^2}\left[\left(i\Lambda - \sum_{i=1}^{N-1}\frac{\partial}{\partial \chi_i}\right)^2 + \frac{1}{4}\right]$$

We notice that the internal Hamiltonian does not account explicitly for the bosonic permutation symmetry of all N particles. For the particles labelled as $1 \ldots N-1$, the symmetry is automatically included as it is equivalent to a simple exchange of the corresponding coordinates t_i, ρ_i, χ_i. However, the exchange of the particles labelled as i and N results in linear transformation of the coordinates t_i and χ_i. Hence, the symmetry with respect to the $i \leftrightarrow N$ exchange is investigated *a posteriori* by defining a "bosonic symmetry factor" Q as the matrix element:

$$Q = \langle \Psi_i | (1 \leftrightarrow N) | \Psi_j \rangle \qquad (1)$$

The Q factor should be unity for true bosonic solutions, being an excellent criteria to evaluate the wavefunction accuracy. We have tested that Q values differs from unity by less than 0.01 (see section S2 of the supporting information).

To calculate the eigenvalues of the internal Hamiltonian, we use the Discrete Variable Representation (DVR) approach[26] as in our previous works.[6, 18, 23] This approach allows an easy and quick evaluation of the interaction potential V_2, with the basis set being obtained as a direct product of functions for the different coordinates. Sinc-DVR functions are conveniently employed for the t and χ coordinates. For the polar radii ρ, however, it is necessary to explicitly treat the singular kinetic energy term $-1/8M\rho_i^2$, arising from the Jacobian transformation to cylindrical coordinates. For this purpose, we use the DVR basis obtained for the finite basis set representation (FBR) built from the radial functions of two-dimensional (2D) Harmonic oscillator functions. However, this basis renders the grid size too large for clusters with N=3 and 4 since the internal Hamiltonian become 7D and 10D, respectively. This problem is solved by using potential-optimized DVR (PO-DVRs) functions[27], allowing for a very fast energy convergence. For instance, bound-state energies are well converged (to within 0.2%) considering just two PO-DVRs for N =3 and 4 (see section S2 of the supporting information).

The diagonalization of the resulting Hamiltonian matrix is performed using the Jacobi-Davidson algorithm.[28] This technique has been very successful even for ill-behaved interactions such as, e.g., the "hard-core" helium cluster interaction problem.[14, 16, 29]

We have obtained the D_2–SWCNT interaction potential $V_1(\rho)$ shown in Fig. 1 (right-hand panel) as a spherical average (thus corresponding to $j = 0$ for the D_2 molecule itself) of our previous *ab initio*-derived potential model.[6] The use of this averaged potential and the corresponding representation of D_2 molecules as point-like particles is justified by the large value of the D_2 rotational constant. For the case of the $H_2 \subset$ SWCNT(10,10) system, we find that the low-lying bound-state energies differ by less than 1.3 cm^{-1} (1%) from those obtained by applying a full treatment of the $j = 0$ state (see Table 1). To model the D_2–D_2 interaction $V_2(r_{ij})$, we use the *ab initio* potential energy surface reported by Hinde[30] as restricted to our one-dimensional model, with the well-depth and position of the potential minimum being 24.72 cm^{-1} and 3.46 Å, respectively. Notice from Fig. 1 that the strength of the D_2–SWCNT interaction is close to two orders of magnitude larger.

The first three bound states of the $D_2 \subset$ SWCNT(11,4) system are shown in Fig. 1 (right panel), with the energies presented in Table 1. Notice the wide amplitude nature of the D_2–SWCNT motion and the large values of the corresponding zero-point energies in Fig. 1 (right

Table 1: Bound-state energies of H_2 and D_2 molecules inside the SWCNT(11,4) and SWCNT(10,10) nanotubes (in cm^{-1}). For the values including the full rotation of the H_2 molecule, see Ref. 23. For $v > 0$, the energies are given relative to $v = 0$.

			H_2	D_2
	Helicity	V_1^{av}	Full rotation $j = 0$	V_1^{av}
$v = 0$	(11,4)	−607.4		−627.0
	(10,10)	−474.1	−475.4	−494.5
$v = 1$	(11,4)	118.0		90.6
	(10,10)	124.2	123.2	94.0
$v = 2$	(11,4)	200.2		164.3
	(10,10)	219.2	218.2	173.3

panel) and Table 1. The density peak position (ca. 2.1 Å from the SWCNT(11,4) center) is slightly larger than the potential minimum location ρ_{min} (ca. 2.0 Å).

Table 2: Bound-state energies of the $(D_2)_2 \subset$ SWCNT(11,4) system (in cm^{-1}). The energies of the excited states are given with respect to that of the ground state. The binding energies are presented in square brackets.

(11,4) SWCNT	
Level	$(D_2)_2$
(0,0,0,0)	−1267.9 [13.9]
(0,0,2,0)	7.1 [6.9]
(0,0,1,2)	7.4 [6.6]
(0,0,2,2)	10.7 [3.3]
(0,0,3,2)	13.0 [0.9]

Table 2 shows the bound-state energies calculated for the $(D_2)_2 \subset$ SWCNT system. The (positive) binding energy ΔE^N is defined as

$$-\Delta E^N = E^N - E^1_{g.s.} - E^{N-1}_{g.s.}$$

with $E^1_{g.s}$ and $E^N_{g.s}$ being the ground-state energies for $N = 1$ and $N - 1$, respectively. The assigned quantum numbers associated to the $(\rho_1, \rho_2, t, \chi)$ coordinates are only indicative since there is a strong mixing between the motions corresponding to the t and χ degrees of freedom. When considering the D_2–SWCNT radial mode, however, it shows up that only the lowest vibrational level $v = 0$ becomes populated and this holds true for any cluster size. Thus, the average D_2–SWCNT interaction for the ground state is just slightly modified from -651 cm^{-1} for $N = 1$ to -659 cm^{-1} for $N = 4$. The average D_2–D_2 interaction per molecular pair ranges from -18 for $N = 2$ to -16 cm^{-1} for $N = 4$, with both values being larger than the free D_2–D_2 dimer counterpart (ca. -13 cm^{-1}). Figure 3 present two-dimensional plots of the ground-state pair densities for three and four D_2 molecules inside the SWCNT(11,4) tube. By considering the cluster geometries associated with their maxima, it becomes clear that three D_2 molecules form an equilateral triangle. From a classical view, this triangle is tunneling between symmetry equivalent potential minima, as illustrated in the left panel of Fig. 3. Our interpretation can be also correlated with a classical analysis of the potential minima landscape. Since the well-depth of the V_1 potential is much larger than the V_2 counterpart, the molecules can be considered as fixed at a distance ρ_{min} from the nanotube axis, where ρ_{min} is the position of the V_1 potential minimum. Then, the rest of the geometry is defined by V_2. On one hand, by requiring that all r_{ij} distances have the values at which the V_2 potential minimum is located, we get $N(N-1)/2$ conditions. On the other hand, we have $2(N-1)$ free internal coordinates since all ρ_i values are fixed to ρ_{min}. Thus, for $N = 2$ and $N = 3$ we have less conditions than variables, and the potential minima landscape corresponds to a 1D constrained curve in the $2(N-1)$ space. This simplified picture explains the reason for the large amplitude motions of the cluster $(D_2)_3$ along and close to

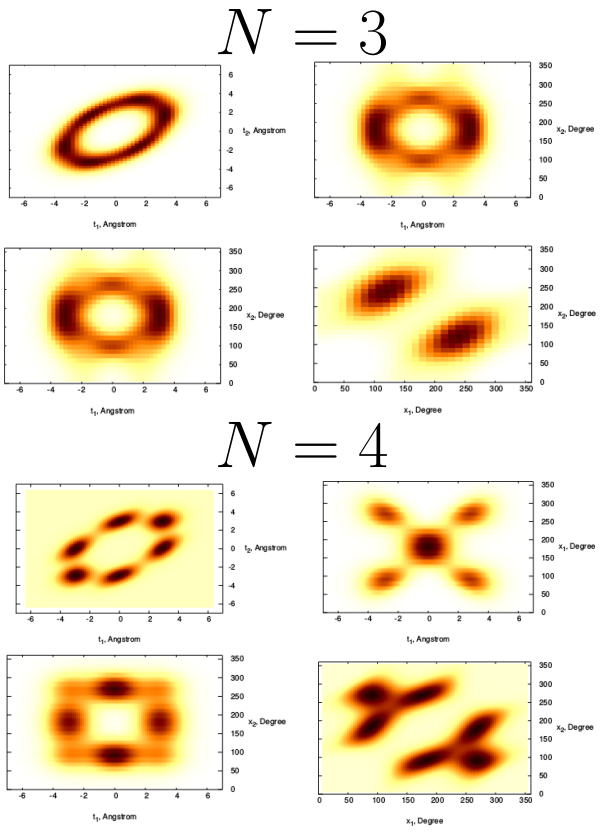

Figure 2: Two-dimensional representation of the pair density as a function of the internal $\chi_{1,2}$ and $t_{1,2}$ coordinates for the ground state of the $(D_2)_3 \subset$ SWCNT (upper panels) and $(D_2)_4 \subset$ SWCNT (bottom panels) systems. The corresponding total energies (binding energies) are -1915.25 (20.4) and -2573.6 (30.1) cm^{-1}, respectively.

this 1D curve, as illustrated in the left panel of Fig. 3. For $N = 4$, the number of variables and conditions is the same so that the potential minimum is just a single point in the parameter space. Accordingly, the pair density is much more compact for $N = 4$ than for $N = 3$, as shown in Fig. 2. As schematically represented in the middle panel of Fig. 3, the four D_2 molecules form a symmetric nearly equilateral pyramidal structure (i.e., a regular tetrahedron) composed by two D_2–D_2 dimers placed centrally inside the SWCNT, and orthogonal to each other and to the SWCNT axis. The mean values of the D_2–SWCNT and D_2–D_2 interactions differ by less than 0.2 cm^{-1} (2%) for N=3 and 4, being consistent with the triangle and equilateral pyramidal structures (see section S3 of the supporting information).

The Z-extension of the pyramidal structure for $N = 4$ is at about 3 Å. Considering the stability of this structure and the fact that the value of V_2 at 6 Å is negligible (ca. -1 cm^{-1}) we can predict that the structure for $N \gg 4$ is a 1D chain of pyramids as shown in the right panel of Fig. 3. This outcome is valid only for this nanotube of 1-nm diameter. It is necessary to consider explicitly more than four molecules to predict the solid-like structure in wider nanotubes. In contrast, three molecules are enough to predict the extended structure in a narrower SWCNT(5,5) tube with a diameter below 1 nm: An aligned 1D molecular chain of D_2 molecules, with the mean D_2–D_2 interaction being essentially that featured by the free dimer (see section S3 of the supporting information).

Finally, aimed to provide further evidence for the transition from a Van der Waals aggregate to a quantum solid, we have investigated the stabilization of the collective rotational motion of a few D_2 molecules. To this end, the lowest-state energies of the $(D_2)_3 \subset (11, 4)$ and the $(D_2)_4 \subset (11, 4)$ systems are represented at each Λ value (the so-called *yrast* states) in Fig. 4. Notice that the line connecting the yrast states (and then termed the yrast line) shows a strong non-monotonic behaviour which is more marked for the $(D_2)_4 \subset (11, 4)$ system. The yrast line for $N = 4$ is reminiscent to that exhibited by electrons and ^{4}He atoms confined in

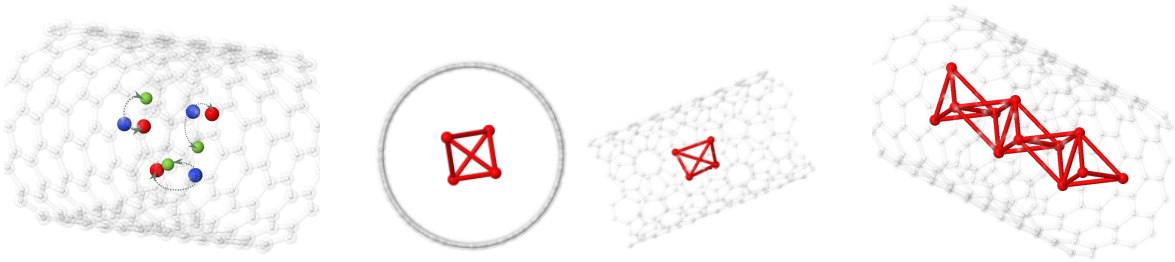

Figure 3: Left hand-panel: Arrangement of three D_2 molecules inside the SWCNT(11,4) nanotube. The spread of the "nuclear" wave functions is indicated by balls (representing molecules) of different colors. Middle panel: Classical structures representing the maximum density arrangements for the ground state of the $(D_2)_4 \subset$ SWCNT system. Right-hand panel: Predicted structure of the $(D_2)_N \subset$ SWCNT system for a large N value. Notice that it bears a clear solid-like high-density appearance.

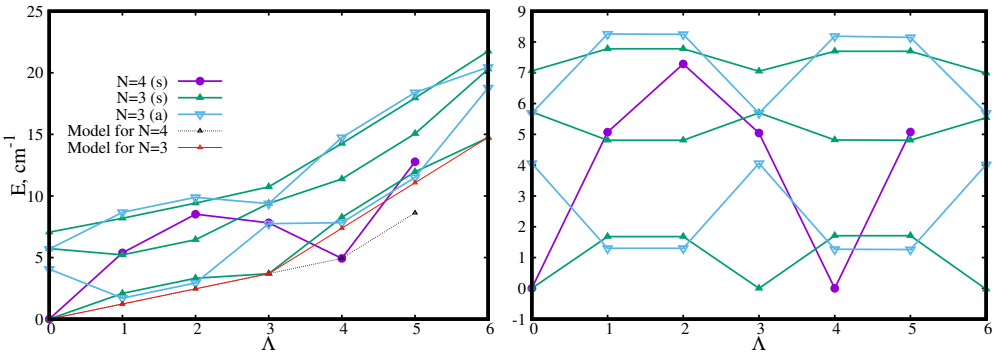

Figure 4: Energies for the lowest-energy states of the $(D_2)_3 \subset (11,4)$ and $(D_2)_4 \subset (11,4)$ systems as a function of Λ. Left-hand panels: total energies. Right hand panels: total energies after removing the overall rotation term $B_{\rm eff}\Lambda^2$. For $N = 3$, The labels s and a indicates that the wave function is symmetric (s) or antisymmetric (a) with respect to the transformation $z \to -z$. The ground state energies obtained with our independent rotational model are also shown (see section S4 of the supporting information).

quantum rings featuring persistent current[31] and persistent flow,[9] respectively.

For the case $N = 3$, the Λ-dependence of the yrast line can be easily explained through an independent rotational model providing energy values agreeing to within 0.2 cm^{-1} with those calculated (see section S4 of the supporting information). This model provides the following explicit expression for the energy as a function of Λ:

$$E(\Lambda) = \frac{B_1}{N}\left[\Lambda^2 + \tilde{\Lambda}(N-\tilde{\Lambda})\right],$$

where $B_1 = \frac{1}{2M\rho_{min}^2}$ and $\tilde{\Lambda} = \mod(\Lambda, N)$. Once the quadratic term is separated, we get the function $B_1\tilde{\Lambda}(N-\tilde{\Lambda})/N$ which is periodic in Λ with period N and symmetric with respect to $\tilde{\Lambda} \to N - \tilde{\Lambda}$. This periodicity can be clearly observed in the right panel of Fig. 4 for all the low-lying states (e.g., the energy values for $\Lambda = 1$ and $\Lambda = 2$ are practically identical). Our finding is similar to that previously observed for helium or para-hydrogen clusters confined by a molecular dopant.[13] In this way, "singularities" at the energy spectrum shown in Fig. 4 are found at $\Lambda = \nu\ N$, with ν integer as a consequence of the bosonic symmetry of the wavefunction. The lowest energy are found when all the bosonic D_2 pseudo-particles bear the same single-particle state. For instance, for

$\Lambda = N = 3$, it occurs when three D_2 molecules occupy the quantum level $m = 1$ (see section S4 of the supporting information).
Importantly, as found for doped para-hydrogen clusters,[13] four deuterium molecules are necessary for the appearance of the collective rotational states as energy minima at $\Lambda = \nu\ N$ with a periodic dependence on Λ. This feature has been previously connected with the onset of a superfluid behaviour and persistent flow in quantum rings made of helium atoms.[9] Using a very simplified but intuitive picture, the rigidity of the structure formed with four D_2 molecules causes that their rotation around the tube axis is collective. We notice that the bosonic symmetry of the wavefunction is a necessary but not a sufficient condition. As shown in Fig. 4, the energy spectrum deviates much from the independent rotational model, already encompassing both bosonic symmetry and periodicity. In fact, as consequence of the hard-core D_2–D_2 interaction, there is a strong mixing between different nuclear modes of the four D_2 molecules. In this way, the energy spectrum resembles that derived for bosonic particles featuring an infinity repulsive interaction when confined in a 1D ring.[32] As predicted for doped hydrogen clusters,[33] this outcome also suggests the "supersolid" character of the cluster formed by four D_2 molecules under confinement. It should be stressed, however, that the same conclusion can be extended to the predicted rigid 1D structure (i.e., through a collective rotational motion of the entangled pyramids with the same phase.)

In concluding, this Letter has been motivated by the identification of the transition from molecular aggregation to a condensed matter system of deuterium at the reduced dimensionality offered by carbon nanotubes. To this end, a highly accurate DVR-based approach has been developed and applied along with a consistently accurate *ab initio*-derived potential model. On one hand, we unambiguously predict the formation of a solid-like pyramidal one-dimensional chain structure. On the other hand, we have demonstrated the strong quantum nature of the formed solid, having features of quantum rings of bosonic particles bearing persistent rotational motion. This important aspect is deduced from full quantum computations and not from the application of a theoretical model. Such advance suggests an important step forward an improved fundamental understanding of hydrogen solid formation in carbon nanotubes for optimized energy storage.

Acknowledgement

We thank Salvador Mirét-Artés (Institute of Fundamental Physics, CSIC) for very helpful discussions. This work has been partly supported by the Spanish Agencia Estatal de Investigación (AEI) and the Fondo Europeo de Desarrollo Regional (FEDER, UE) under Grant No. MAT2016-75354-P. The CESGA supercomputer center (Spain) and the CTI (CSIC) are acknowledged for having provided the computational resources.

Supporting Information available: Complementary details on: (1) the *ab initio*-derived potential model; (2) basis sets used in the calculations of the wavefunctions characterizing the deuterium clusters motion; (3) the partition of the energy into deuterium-nanotube and deuterium-deuterium interaction; (4) the independent rotational model.

References

(1) Cazorla, C.; Boronat, J. Simulation and Understanding of Atomic and Molecular Quantum Crystals.*Rev. Mod. Phys.* **2017**, *89*, 035003.

(2) Rossi, M.; Ancilotto, F. Superfluid Behavior of Quasi-One-Dimensional p-H_2 Inside a Carbon Nanotube.*Phys. Rev. B* **2016**, *94*, 100502.

(3) Ferré, G.; Gordillo, M. C.; Boronat, J. Luttinger Parameter of Quasi-One-Dimensional para$-H_2$.*Phys. Rev. B* **2017**, *95*, 064502.

(4) Del Maestro, A.; Boninsegni, M. Absence of Superfluidity in a Quasi-One-Dimensional Parahydrogen Fluid Adsorbed Inside Carbon Nanotubes.*Phys. Rev. B* **2017**, *95*, 054517.

(5) Ting, V. P.; Ramirez-Cuesta, A. J.; Bimbo, N.; Sharpe, J. E.; Noguera-Diaz, A.; Presser, V.; Rudic, S.; Mays, T. J. Direct Evidence for Solid-like Hydrogen in a Nanoporous Carbon Hydrogen Storage Material at Supercritical Temperatures.*ACS Nano* **2015**, *9*, 8249–8254.

(6) De Lara-Castells, M. P.; Hauser, A. W.; Mitrushchenkov, A. O.; Fernández-Perea, R. Quantum Confinement of Molecular Deuterium Clusters in Carbon Nanotubes: *Ab Initio* Evidence for Hexagonal Close Packing.*Phys. Chem. Chem. Phys.* **2017**, *19*, 28621–28629.

(7) Hauser, A. W.; de Lara-Castells, M. P. Carbon Nanotubes Immmersed in Superfluid Helium: The Impact of Quantum Confinement on Wetting and Capillary Action.*J. Phys. Chem. Lett.* **2016**, *7*, 4929–4935.

(8) Hauser, A. W.; Mitrushchenkov, A. O.; de Lara-Castells, M. P. Quantum Nuclear Motion of Helium and Molecular Nitrogen Clusters in Carbon Nanotubes.*J. Phys. Chem. C* **2017**, *121*, 3807–3821.

(9) Bloch, F. Superfluidity in a Ring.*Phys. Rev. A* **1973**, *7*, 2187–2191.

(10) Grebenev, S.; Sartakov, B. G.; Toennies, J. P.; Vilesov, A. F. Spectroscopic Investigation of OCS $(p\text{-}H_2)_n$ (n =1–16) Complexes Inside Helium Droplets: Evidence for Superfluid Behavior.*J. Chem. Phys.* **2010**, *132*, 064501.

(11) Grebenev, S.; Sartakov, B.; Toennies, J. P.; Vilesov, A. F. Evidence for Superfluidity in Para-Hydrogen Clusters Inside Helium-4 Droplets at 0.15 Kelvin.*Science* **2000**, *289*, 1532–1535.

(12) Li, H.; Le Roy, R. J.; Roy, P.-N.; McKellar, A. R. W. Molecular Superfluid: Nonclassical Rotations in Doped Para-Hydrogen Clusters.*Phys. Rev. Lett.* **2010**, *105*, 133401.

(13) De Lara-Castells, M. P.; Mitrushchenkov, A. O. Collective Bosonic Excitations in Doped para-H_2 Clusters through the Full-Configuration-Interaction Nuclear Orbital Approach.*J. Phys. Chem. Lett.* **2011**, *2*, 2145–2151.

(14) De Lara-Castells, M. P.; Delgado-Barrio, G.; Villarreal, P.; Mitrushchenkov, A. O. A Full-Configuration Interaction "Nuclear Orbital" Method to Study Doped ^3He_N Clusters ($N \leq 4$).*J. Chem. Phys.* **2006**, *125*, 221101.

(15) De Lara-Castells, M. P.; Delgado-Barrio, G.; Villarreal, P.; Mitrushchenkov, A. O. An Optimized Full-Configuration-Interaction Nuclear Orbital Approach to a Hard-Core Interaction Problem: Application to $(^3He)_N$–Cl_2(B) Clusters.*J. Chem. Phys.* **2009**, *131*, 194101.

(16) De Lara-Castells, M. P.; Aguirre, N. F.; Villarreal, P.; Barrio, G. D.; Mitrushchenkov, A. O. Quantum Solvent States and Rovibrational Spectra of Small Doped ^{3}He Clusters Through the Full-Configuration-Interaction Nuclear Orbital Approach: The $(^3He)_N$–Cl_2(X) case ($N \leq 4$).*J. Chem. Phys.* **2010**, *132*, 194313.

(17) Aguirre, N. F.; Villarreal, P.; Delgado-Barrio, G.; Mitrushchenkov, A. O.; de Lara-Castells, M. P. Solvent States and Spectroscopy of Doped Helium Clusters as a Quantum-Chemistry-like Problem.*Phys. Chem. Chem. Phys.* **2013**, *15*, 10126–10140.

(18) Hauser, A. W.; Mitrushchenkov, A. O.; de Lara-Castells, M. P. Quantum Nuclear Motion of Helium and Molecular Nitrogen Clusters in Carbon Nanotubes.*J. Phys. Chem. C* **2017**, *121*, 3807–3821.

(19) De Lara-Castells, M. P.; Bartolomei, M.; Mitrushchenkov, A. O.; Stoll, H. Transferability and Accuracy by Combining Dispersionless Density Functional and Incremental Post-Hartree-Fock Theories: Noble Gases Adsorption on Coronene/Graphene/Graphite Surfaces.*J. Chem. Phys.* **2015**, *143*, 194701.

(20) De Lara-Castells, M. P.; Hauser, A. W.; Mitrushchenkov, A. O. Ab Initio Confirmation of a Harpoon-Type Electron Transfer in a Helium Droplet.*J. Phys. Chem. Lett.* **2017**, *8*, 4284–4288.

(21) Misquitta, A. J.; Podeszwa, R.; Jeziorski, B.; Szalewicz, K. Intermolecular Potentials Based on Symmetry-Adapted Perturbation Theory with Dispersion Energies from Time-Dependent Density-Functional Calculations.*J. Chem. Phys.* **2005**, *123*, 214103.

(22) Heßelmann, A.; Jansen, G.; Schütz, M. Density-Functional-Theory Symmetry-Adapted Intermolecular Perturbation Theory with Density Fitting: A New Efficient Method to Study Intermolecular Interaction Energies.*J. Chem. Phys.* **2005**, *122*, 014103.

(23) De Lara-Castells, M. P.; Mitrushchenkov, A. O. Spectroscopy of a Rotating Hydrogen Molecule in Carbon Nanotubes.*Phys. Chem. Chem. Phys.* **2019**, *21*, 3423–3430.

(24) De Lara-Castells, M. P.; Mitrushchenkov, A. O. Nuclear Bound States of Molecular Hydrogen Physisorbed on Graphene: An Effective Two-Dimensional Model.*J. Phys. Chem. A* **2015**, *119*, 11022–11032.

(25) Bartolomei, M.; Perez de Tudela, R.; Arteaga, K.; González-Lezana, T.; Hernandez, M. I.; Campos-Martınez, J.; Villarreal, P.; Hernández-Rojas, J.; Breton, J.; Pirani, F. Adsorption of Molecular Hydrogen on Coronene with a New Potential Energy Surface.*Phys. Chem. Chem. Phys.* **2017**, *19*, 26358–26368.

(26) Bačic, Z.; Light, J. C. Theoretical Methods for Rovibrational States of Floppy Molecules.*Annu. Rev. Phys. Chem.* **1989**, *40*, 469–498.

(27) Echave, J.; Clary, D. C. Potential Optimized Discrete Variable Representation.*Chem. Phys. Lett.* **1992**, *190*, 225–230.

(28) Sleijpen, G. L. G.; der, H. A. V. A Jacobi–Davidson Iteration Method for Linear Eigenvalue Problems.*SIAM J. Matrix Anal. Appl.* **1996**, *17*, 401–425.

(29) De Lara-Castells, M.; Mitrushchenkov, A.; Delgado-Barrio, G.; Villarreal, P. Using a Jacobi-Davidson "Nuclear Orbital" Method for Small Doped ^{3}He Clusters.*Few-Body Systems* **2009**, *45*, 233–236.

(30) Hinde, R. J. A Six-Dimensional H_2-H_2 Potential Energy Surface for Bound State Spectroscopy.*J. Chem. Phys.* **2008**, *128*, 154308.

(31) Viefers, S.; Koskinen, P.; Singha Deo, P. S.; Manninen, M. Quantum Rings for Beginners: Energy Spectra and Persistent Currents.*Physica E Low Dimens. Syst. Nanostruct.* **2004**, *21*, 1–35.

(32) Manninen, M.; Viefers, S.; Reimann, S. Quantum Rings for Beginners II: Bosons Versus Fermions.*Physica E Low Dimens. Syst. Nanostruct.* **2012**, *46*, 119–132.

(33) Mezzacapo, F.; Boninsegni, M. On the Possible "Supersolid" Character of Parahydrogen Clusters.*J. Phys. Chem. A* **2011**, *115*, 6831–6837.